Article

Quantum precision measurement of two-dimensional forces with 10^{-28}-Newton stability

Xinxin Guo [a,1], Zhongcheng Yu [a,1], Fansu Wei [a], Shengjie Jin [a], Xuzong Chen [a], Xiaopeng Li [b,c,d,e,*], Xibo Zhang [f,*], Xiaoji Zhou [a,g,*]

[a] *State Key Laboratory of Advanced Optical Communication System and Network, School of Electronics, Peking University, Beijing 100871, China*
[b] *State Key Laboratory of Surface Physics, Key Laboratory of Micro and Nano Photonic Structures (MOE), and Department of Physics, Fudan University, Shanghai 200433, China*
[c] *Institute for Nanoelectronic Devices and Quantum Computing, Fudan University, Shanghai 200433, China*
[d] *Shanghai Qi Zhi Institute, AI Tower, Xuhui District, Shanghai 200232, China*
[e] *Shanghai Research Center for Quantum Sciences, Shanghai 201315, China*
[f] *International Center for Quantum Materials, School of Physics, Peking University, Beijing 100871, China*
[g] *Institute of Advanced Functional Materials and Devices, Shanxi University, Taiyuan 030031, China*

ARTICLE INFO

ABSTRACT

High-precision sensing of vectorial forces has broad impact on both fundamental research and technological applications such as the examination of vacuum fluctuations and the detection of surface roughness of nanostructures. Recent years have witnessed much progress on sensing alternating electromagnetic forces for the rapidly advancing quantum technology—orders of magnitude improvement has been accomplished on the detection sensitivity with atomic sensors, whereas such high-precision measurements for static electromagnetic forces have rarely been demonstrated. Here, based on quantum atomic matter waves confined by a two-dimensional optical lattice, we perform precision measurement of static electromagnetic forces by imaging coherent wave mechanics in the reciprocal space. The lattice confinement causes a decoupling between real-space and reciprocal dynamics, and provides a rigid coordinate frame for calibrating the wavevector accumulation of the matter wave. With that we achieve a state-of-the-art sensitivity of $2.30(8) \times 10^{-26}$ N/$\sqrt{\text{Hz}}$. Long-term stabilities on the order of 10^{-28} N are observed in the two spatial components of a force, which allows probing atomic Van der Waals forces at one millimeter distance. As a further illustrative application, we use our atomic sensor to calibrate the control precision of an alternating electromagnetic force applied in the experiment. Future developments of this method hold promise for delivering unprecedented atom-based quantum force sensing technologies.

1. Introduction

Measuring force with high-precision has been attracting continuous efforts in the interest of fundamental science discoveries and advancing technological applications [1]. It plays a vital role in fundamental physics tests ranging from examination of vacuum fluctuation mediated Casimir forces [2–4] and atomic scale nanofrictions [5] to detecting gravitational waves [6,7] and string theory with extra dimensions [8]. It is also key to high-precision technologies such as atomic-resolution microscopy [9–12] and frontier nanoscale fabrication [13]. The recently upgraded SI mass unit from the macroscopic standard to the fundamental Planck constant ($\hbar$) base [14] creates new demands on implementation of high-precision force measurement with quantum mechanical technologies.

As force is inherently tied to the mechanical motion in real space, high-precision force measurement has primarily relied on real space protocols, whose standard quantum limit (SQL)

$$\delta F_{\text{real}} \sim (m\hbar/\Delta T^3)^{1/2}, \qquad (1)$$

has been established for a force F acting on a free mass m for a time duration ΔT [15]. This SQL is unavoidable for mechanical motion based measurements [16]. The key to reaching high precision is to fabricate a miniaturized sensor with extremely small mass and ultralow defect density, and at the same time maintain a high level of signal-to-noise ratio [1]. In recent years, there has been much research effort devoted to optimizing nanoscale opto-mechanical devices [17–23] and quantum atomic gases [24–29] for high preci-

* Corresponding authors.
  E-mail addresses: xiaopeng_li@fudan.edu.cn (X. Li), xibo@pku.edu.cn (X. Zhang), xjzhou@pku.edu.cn (X. Zhou).
[1] These authors contributed equally to this work.

sion force sensing. With nanoscale opto-mechanical devices in a cryogenic environment, a force measurement sensitivity of a few times 10^{-21} N/$\sqrt{\text{Hz}}$ has been achieved [19,20]. The atomic gas system provides an approach of quantum force sensing using a large number of microscopically identical force sensors, namely the atoms. With atomic sensors, a measurement sensitivity of about 3.5×10^{-26} N/$\sqrt{\text{Hz}}$ has been reached for alternating (a.c.) forces [24,26]. For static (d.c.) electromagnetic forces, a measurement sensitivity of 10^{-19} N/$\sqrt{\text{Hz}}$ has been reported based on the mechanical response of a three-dimensional trapped ion sensor [29]. The technology for quantum precision measurement of d.c. electromagnetic force demands further developments for enhancing the sensitivity. For an atomic Bose–Einstein condensate (BEC), an external force applied to the system produces a macroscopic quantum state of matter wave, developing a wavevector-to-force response apart from the spatial motion. This quantum phenomenon has been observed for alkali metal atomic matter waves with persisting quantum coherence [30–32]. The BEC confined in a one-dimensional lattice has been applied to measure the earth gravity along one fixed dimension [33,34]. Quantum interference of cold atoms has also been utilized to perform precision measurement of magnetic field gradient [35–37]. Here, we perform precise sensing of a two-dimensional force by separating the wavevector-to-force response from the real-space dynamics using a two-dimensional optical lattice, such that the spatial motion is suppressed to minimize potential systematic errors without compromising the detection signal-to-noise ratio. This sets our force measurement free from the type of SQL in Eq. (1), and we thereby accomplish a sensitivity of $2.30(8) \times 10^{-26}$ N/$\sqrt{\text{Hz}}$ in the measurement of two-dimensional d.c. electromagnetic forces. With such high measurement sensitivity, long-term stabilities of $1.7^{+1.3}_{-0.4} \times 10^{-28}$ and $6.3^{+1.2}_{-0.7} \times 10^{-28}$ N for the two spatial components of a vectorial force are demonstrated based on consecutive experimental runs for 3×10^5 s. The measurement precision for weak electromagnetic forces is sufficiently high such that an alternating force can be well controlled and measured in our experiment. Our results represent a significant step forward in the precision of force sensing, potentially promoting the force-based fundamental physics discoveries and technological applications, including testing vacuum fluctuations [2–4] and performing remote surface tomography by probing atomic Van der Waals forces [27].

2. Methods

2.1. Decoupling the real- and reciprocal-space dynamics with a light-crystal matter wave

Our experiment is based on an atomic BEC confined by a triangular two-dimensional optical lattice (Fig. 1). Details of our atom trap have been described in our previous experimental works [38,39]. We take each atom as an individual force sensor and implement the impulse-momentum theorem

$$\vec{F} = \frac{\vec{q}_f - \vec{q}_i}{\Delta T}, \tag{2}$$

for quantum force sensing. Here $\vec{q}_i$ ($\vec{q}_f$) is the initial (final) quasi-momentum of each atom in the light crystal, and ΔT is the time duration of the force acting on the BEC. As ΔT can be accurately controlled in the experiment, high precision force sensing is then reduced to detecting quasi-momentum. Having a BEC in equilibrium to start with, the momentum is zero initially, and remains vanishing in the absence of an external force, which corresponds to a background-free force measurement (Fig. 1b). Because of the wave mechanical nature of a BEC, the quasi-momentum response

under an external force can be detected by measuring the wavevector $\vec{k}_f$ of the matter wave ($\vec{k}_f = \vec{q}_f / \hbar$), which, in sharp contrast to conventional mechanical schemes [1,15,24,26,29], no longer requires probing real-space motion. The wavevector is precisely detectable in the experiment because the atoms in the matter wave form a macroscopic quantum state sharing the same quasi-momentum, giving rise to a sharp Bragg peak in the reciprocal space (Fig. 1a4).

One novel aspect with our light crystal BEC sensing is the decoupling of reciprocal-space dynamics from the real-space mechanical motion. The precision force sensing solely relies on the differential wavevector measurements and the fundamental Planck constant. The wavevector measurement can be precisely calibrated according to the first Brillouin zone (FBZ), a natural reference frame of the reciprocal space provided by the rigid light crystal (Fig. 1c). With our BEC force sensor, the fundamental limitation on the force measurement precision is from the quantum shot noise in the atomic quasi-momentum caused by the shallow harmonic trap,

$$\delta F_{\text{reciprocal}} \sim \frac{\hbar}{\sqrt{N_0} \Delta T \times l_Q}, \tag{3}$$

with l_Q a characteristic length scale of the BEC, and N_0 the number of condensed atoms (see the Supplementary materials for more details). The measurement scheme is free of such demanding experimental techniques as superresolution imaging or velocimetry as in real-space mechanical motion techniques. Our $\delta F_{\text{reciprocal}}$ is independent of atomic mass and insensitive to spatial position, velocity or their technical fluctuations. This scheme then avoids the constraint by the well celebrated SQL for real-space motion based protocols [1,15,24,26,29]. Moreover, with the atoms strongly confined by the light crystal, the real-space atomic motion is strongly suppressed. A triangular lattice is chosen because it has a relatively smaller bandwidth, and consequently leads to a smaller group velocity for the atoms, as compared to the square lattice having the same lattice depth (see the Supplementary materials for more details). For the force sensing, such strong suppression minimizes the systematic errors caused by initial position drift in measuring the atomic quasi-momentum after a time-of-flight process (see the Supplementary materials for more details). In our experiment, we choose a moderate time duration ΔT so as to keep the BEC within the first Brillouin zone. Allowing the BEC to move across the Brillouin zone boundary in the two-dimensional force measurement would result in the complexity of analyzing the BEC moving trajectory across the two-dimensional Brillouin zone, which is in sharp contrast to the one-dimensional force measurement using multiple cycles of Bloch oscillations [33,34]. The resultant force sensitivity as measured in our experiment reaches $2.30(8) \times 10^{-26}$ N/$\sqrt{\text{Hz}}$, with both the measurement time and the BEC preparation time included in the definition of the measurement sensitivity. Furthermore, when considering the force acting time of $\Delta T \approx 4$ ms only, we obtain a force measurement sensitivity of 1.7×10^{-28} N/$\sqrt{\text{Hz}}$, reaching significantly beyond the SQL for the mechanical force measurement [15] of 9×10^{-28} N/$\sqrt{\text{Hz}}$ (using Eq. (1)) under the same measurement time.

2.2. Experimental setup to reach long-term high stability

In the experiment we have a laser-produced triangular light crystal that spans across the x–y plane (Fig. 2a), with the y-direction (vertical) along the earth gravity [40,41]. The atomic gas is thus confined in a two-dimensional array of tubes elongated along the z-direction. The atomic density in the tube is tunable. This allows to maintain sufficiently weak interaction, which would
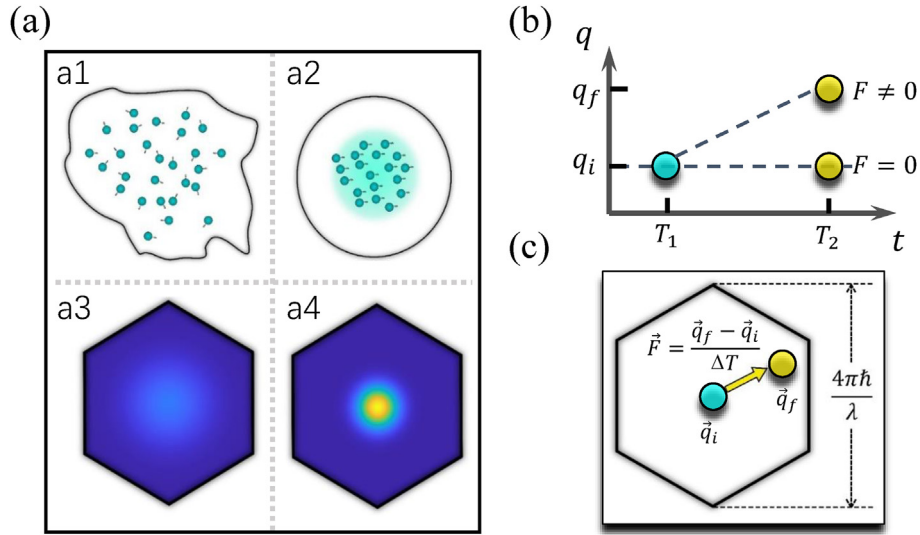
Fig. 1. (Color online) High-precision force measurement by atomic BEC. (a) Illustration of how quantum coherence enhances sensitivity. More thermal atoms (a1) cause a momentum distribution broadening (a3) and add thermal noise to force sensing; whereas more atoms in a BEC (a2) improve the signal-to-noise ratio due to quantum coherence (a4). (b) Wavevector accumulation of the quantum atomic matter wave under an external force. (c) The reciprocal space of a triangular light crystal formed by laser. The size and boundary of the first Brillouin zone, as determined by the laser wavelength (λ) and orientation geometry, define a rigid two-dimensional coordinate frame for precise measurement of atomic wavevector.

otherwise cause decoherence in the wave dynamics and a consequent limitation on the measurement time. Our BEC contains about 2×10^5 atoms, which is prepared in a hybrid trap formed by a combination of quadrupole magnetic, optical dipole, and gravitational potentials as described in our previous works [38,39]. The system is then loaded into a triangular light crystal created by three laser beams intersecting at $120°$ angles, forming a two-dimensional array of tubes. The laser wavelength is $\lambda = 1064$ nm, and the resultant lattice spacing is $2\lambda/3$. This 2D triangular optical lattice is slowly ramped to its final depth V_0 in a ramping time of 80 ms such that the BEC is loaded into the ground energy band of the lattice with a loading efficiency typically above 98%.

We apply external forces in the x–y plane after preparation of the BEC system. To demonstrate the generality of our BEC force sensing, we implement both optical and magnetic forces (see the Supplementary materials for more details), to be referred to as $\vec{F}_o$ and $\vec{F}_m$, respectively. After the force is fully applied, we shut off all traps, and let the atoms expand for 31 ms, namely time-of-flight (TOF), before performing the absorption imaging. We measure the wavevector of the generated matter wave by time-of-flight imaging (see the Supplementary materials for more details). By introducing feedback control of laser intensity and magnetic coil currents to afford a large number of measurement cycles, the forces are maintained stable for consecutive experimental runs over a long-term period of several days. We also make efforts on holding the stability of experimental conditions such as room temperature and humidity to our best capability. Based on the experiment designing principle in Eq. (2), our measurements are insensitive to the fluctuations of atom number, lattice depth, and optical phases, some of which can be difficult to control precisely.

3. Results and discussion

3.1. The long-term stability

By varying the force acting time ΔT, we measure how the wavevector of the matter wave accumulates in its dynamics. The results are shown in Fig. 2b. The observed linear relationship

confirms that the experimental noise is well under control such that the momentum impulse theorem (Eq. (2)) indeed applies to the BEC wave dynamics. The vectorial forces—both of the magnitude and the direction—can then be reliably extracted either by fitting the realtime wavevector accumulation or by calculating the difference between the initial and final points. We proceed by performing a differential wavevector measurement according to the second approach that only requires two experimental cycles taking about $\tau_0 \approx 76$ s. Because the BEC preparation time (about 38 s) is much longer than the force acting time (4 ms), the time for one force measurement is essentially two times of the BEC preparation time. The inset of Fig. 2b illustrates how we extract the force from the TOF measurements. The force is determined by measuring the quasi-momentum difference $\Delta \vec{q} = \vec{q}_f - \vec{q}_i$ between T_1 and T_2. The quasi-momentum measurement is performed by averaging over the zeroth order momentum peak in the TOF. The higher-order momentum peaks provide a rigid coordinate frame to accurately calibrate the quasi-momentum, as the distance between two adjacent momentum peaks corresponds to a momentum scale of $\frac{2\sqrt{3}\pi\hbar}{\lambda}$.

We determine the long-term stability of the force measurement by collecting a large amount of experimental data. Fig. 2c and d show two groups of measurements corresponding to optical and magnetic forces applied along a direction slightly deviated from the y axis. By analyzing the results in Fig. 2c1, d1, we find the data points collected over a long period of time—several days for the optical force—obey a standard normal distribution (Fig. 2c2, c3, d2, d3). This implies there is no serious long-term drift in our experiment, because otherwise the distribution can develop a structure of multiple peaks or a flattened plateau in the middle. More systematically, the long-term stability is characterized by the Allan Deviation (ADEV) as a function of data averaging time τ_1 [1] as shown in Fig. 2c4 and d4. It is evident from the ADEV of x-component of the optical force $F_{o,x}$ that our force sensing remains stable up to tens of thousands of seconds, where the consecutive measurement fluctuations are dominated by white noise. With the high sensitivity by our BEC force sensor, we reach a long-term stability $\delta F_{o,x} = 1.7^{+1.3}_{-0.4} \times 10^{-28}$ N (Fig. 2c4). For the y-component, the ADEV has a slightly different behavior. It shows an upward bending behavior after τ_1 exceeds a certain characteris-
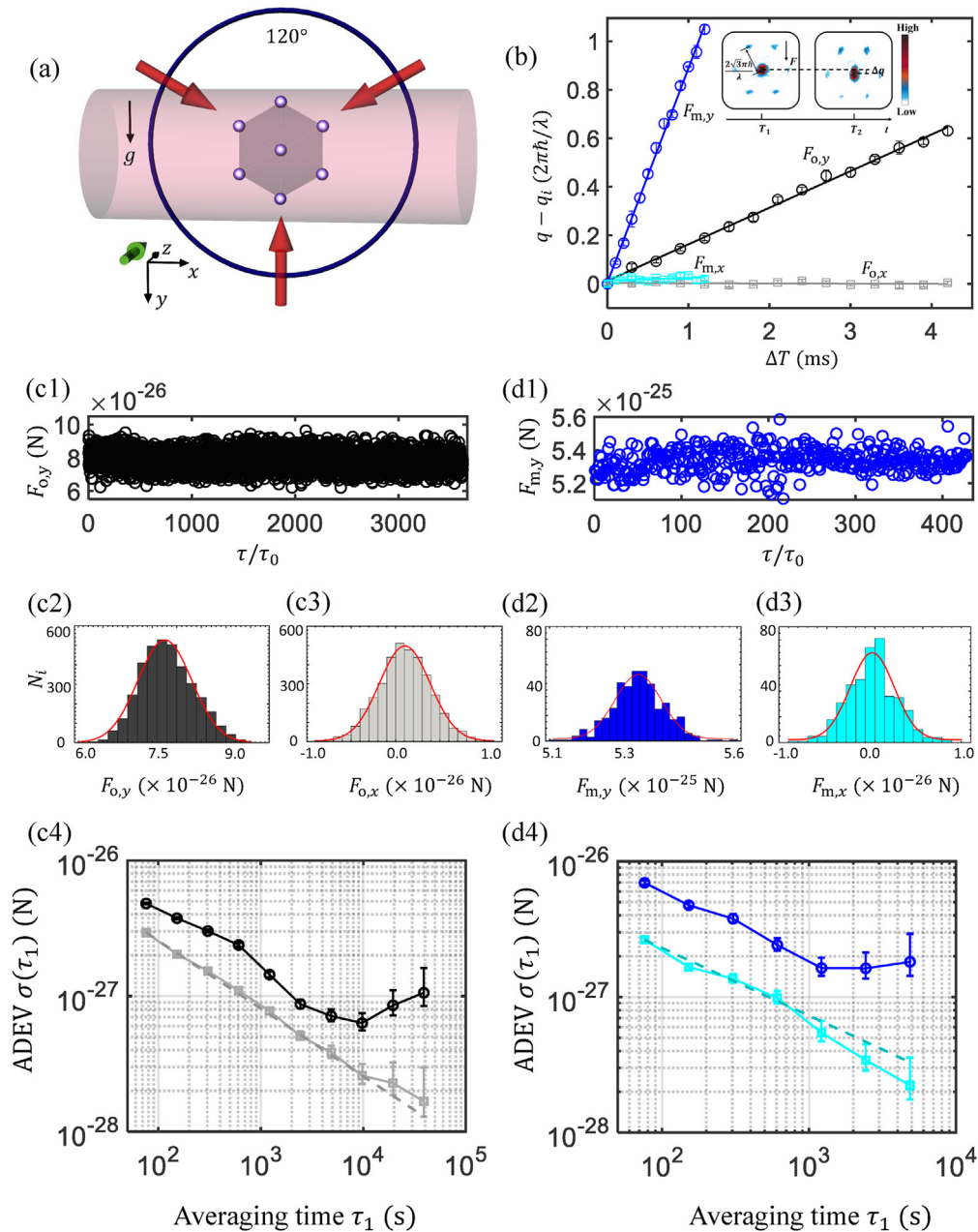
Fig. 2. (Color online) High-precision measurement of static electromagnetic forces in two dimensions. (a) The orientation of the atomic array confined by the triangular light crystal in the x–y plane. The horizontal pink cylinder illustrates the optical dipole trap in our experiment. The system is probed by an imaging laser beam (green arrow) along the $\hat{z}$ direction. (b) Measurement of atomic wave evolution upon static forces. Two types of forces, optical ($\vec{F}_o$) and magnetic ($\vec{F}_m$), have been implemented. The wavevector of the BEC shows a linear dependence on the force acting time ΔT. The error bars represent the standard error averaging over five experimental runs. Inset shows images of atomic momentum distribution at different evolution times. The sub-figure on the left is the TOF image with zero acting time of an external force. Here, for a BEC in a 2D optical lattice, the atoms are distributed over several momentum peaks, and the distance between two adjacent momentum peaks is $\frac{2\sqrt{3}\pi\hbar}{\lambda}$. The sub-figure on the right is a TOF image with finite acting time of the external force, where the BEC momentum accumulates along the direction of the external force. (c) and (d) correspond to the experimental results on measuring the optical and magnetic forces, respectively. Here τ is the total experimental time and $\tau_0 \approx 76$ s is the time cost for a single data point. (c1) and (d1) present the raw data for the y-component forces. (c2, c3, d2, d3) provide the histogram analysis of the measurements of the two spatial components of the forces. (c4) and (d4) show the Allan deviation (ADEV) as a function of the averaging time (τ_1), with error bars representing 1σ statistical uncertainty. The grey and black (light blue and blue) colors illustrate x- and y-components of the optical (magnetic) force. As a reference, the dashed lines mark a scaling of an ADEV with the averaging time τ_1 as $1/\sqrt{\tau_1}$.

tic time. Owing to the difference between the x- and y-directions (axial and radial directions for the dipole trap shown in Fig. 2a), we consider the $1/\sqrt{\tau_1}$ scaling of the x-component instability as revealing the measurement performance of BEC force sensing, and attribute the higher instability in the y-component, particularly at a time scale of 10^4 and 10^3 s respectively for optical and magnetic forces, to the non-white-noise instabilities in the applied

force, potentially originating from the long-term laser beam pointing fluctuations caused by certain thermal-noise-induced drift of our apparatus. The two components of the optical force are determined as $F_{o,x} = 1.0(2) \times 10^{-27}$ N and $F_{o,y} = 7.81(6) \times 10^{-26}$ N, and the direction angle of the force with respect to the y-axis is determined as $\theta_o = (0.013 \pm 0.002)$ radian. For the magnetic force, we measure $F_{m,x} = -2(2) \times 10^{-28}$ N, and $F_{m,y} = (5.336 \pm 0.016) \times$

10^{-25} N, $\theta_m = -4(4) \times 10^{-4}$ radian, correspondingly. As a crosscheck, we also show the force stabilities by the technique of binning the experimental data and analyzing the corresponding histogram [42], and the results are comparable to the ADEV analysis (see the Supplementary materials for more details).

3.2. Sensitivity of the BEC force sensor

We extract the measurement sensitivity from the ADEV by taking the ADEV averaging time $\tau_1 = \tau_0$ (see the Supplementary materials for more details). For the optical force with $\Delta T = 4.2$ ms, we determine a sensitivity for the x and y components, $S_{o,x} = 2.56(3) \times 10^{-26}$ N/$\sqrt{\text{Hz}}$, and $S_{o,y} = 4.20(5) \times 10^{-26}$ N/$\sqrt{\text{Hz}}$, with both the measurement and BEC preparation times included. For the magnetic force whose magnitude is relatively larger, we choose $\Delta T = 3.6$ ms, and measure a sensitivity $S_{m,x} = 2.30(8) \times 10^{-26}$ N/$\sqrt{\text{Hz}}$, and $S_{m,y} = 6.1(2) \times 10^{-26}$ N/$\sqrt{\text{Hz}}$. The BEC sensor thus demonstrates a high sensitivity on the 10^{-26} N/$\sqrt{\text{Hz}}$ level for measuring two-dimensional electromagnetic forces, which shows significant improvement over previous d.c. measurements of vectorial electromagnetic forces based on mechanical responses [23,29].

From Eq. (3), the force sensitivity is expected to improve further upon increasing measurement time as $1/\Delta T$, in the regime where the BEC preparation time dominates over the measurement time. This scaling is confirmed in our experiment (Fig. 3) for both spatial components of a force. It is natural to improve the force sensitivity

by increasing the measurement time or reducing the BEC preparation time. The preparation time is about 38 s in our experiment, which can be readily reduced to a few seconds with advanced cold atom technology, for example by dynamically reducing the trap size [43]. It is less trivial to increase the measurement time because this is limited by the interaction induced decoherence. That would require using a different atomic species whose interactions are negligible or can be tuned by Feshbach resonances. Having the interaction shut off, for example with ^{133}Cs or ^{88}Sr atoms, we expect the measurement time can reach the order of ten seconds [30], and the sensitivity would then be improved by another three orders of magnitude. Turning off the interaction would also make the quasi-momentum peak sharper as it removes the quasi-momentum broadening induced by quantum depletion (more details in Supplementary materials). Once the interaction is off, the sensitivity can also be improved further by increasing the atom number, for which the improvement scales as $\sqrt{N_0}$. Although our measured sensitivity has exceeded the SQL established for mechanical schemes, there is still quite some room for us to improve the technicality. Fig. 3 shows the computed quantum limit (QL) of our quantum wave mechanical measurement, which is about a factor of 80 smaller than the measured sensitivity of $F_{o,x}$. This can be attributed to residual experimental imperfections such as fluctuations in the trapping potential and environmental temperatures and humidity. Taking all these potential improvements into account, realizing a measurement beyond a 10^{-30} N stability is anticipated in the near term with the BEC force sensing scheme.

3.3. Calibrating alternating electromagnetic forces by BEC sensor

BEC force sensing provides novel opportunities for atomic quantum sensors. The realized high measurement stability allows prob-
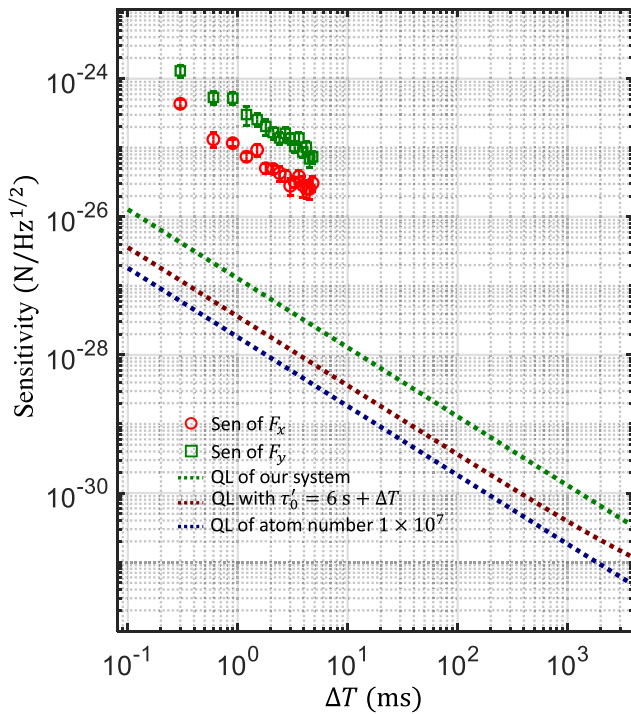

Fig. 3. (Color online) The sensitivity of force measurement under varying experimental conditions. The red circles and green squares correspond to the experimentally determined sensitivities for x- and y-components of the optical force with various force acting times (ΔT). Error bars represent 1σ statistical uncertainties. The green dotted line is the theoretical quantum limit (QL) of the sensitivity calculated by taking the implemented experimental condition, which is proportional to $1/\Delta T$ as the BEC preparation time dominates over the force acting time in our experiment. The blue and brown dotted lines indicate quantum limits for an increased atom number (10^7) and for a reduced BEC preparation time of (3 s), respectively.
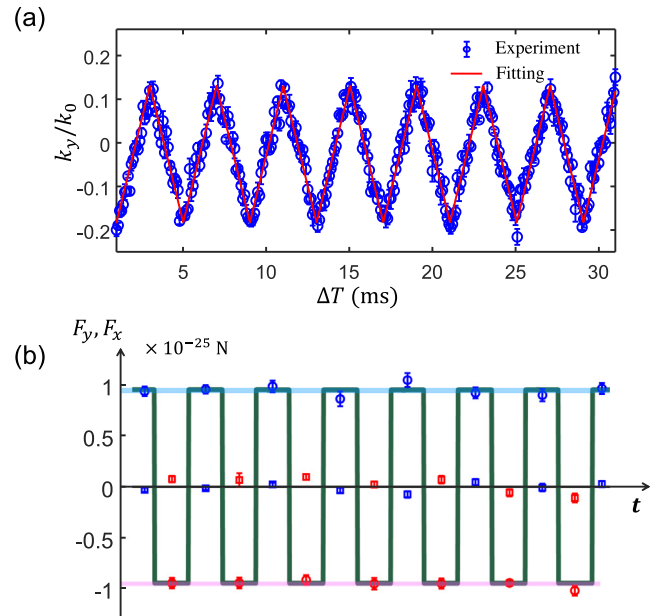

Fig. 4. (Color online) BEC sensing of alternating electromagnetic forces in two dimensions. (a) Measurement of atomic wave evolution upon alternating forces along the y-direction. Blue spheres represent the experiment measurements data, and the error bars represent the standard error averaging over five independent experiment runs. Red solid lines represent the fitting of the experimental data. (b) Experimental results on measuring the alternating electromagnetic force. The Blue spheres (red spheres) represent the measurements of y-components of the alternating force. Blue squares (red squares) represent the measurements of x-components of the alternating force. Dark green line is a guide-to-the-eye that illustrates the periodicity for modulating the y-component of the force.

ing atomic Van der Waals forces at a millimeter distance [27], which would enable unprecedented atom force based quantum sensing technology. As an illustrative application, we use the BEC sensor to calibrate the control precision of the electromagnetic forces applied to the atomic systems in the experiment. By periodically changing the intensity of the external optical dipole trap (Fig. 4), we deliberately apply a square-wave modulation in the *y*-component of the force on the BEC. Atoms in the BEC sensor exhibit an oscillating wavevector of a triangular wave form. Fig. 4a gives the accumulation of the *y*-component wavevector of the matter wave with different force acting time ΔT. The oscillating frequency of the wavevector is determined to be 250 Hz. The applied forces at each plateau of the square wave are extracted by fitting the experimental results of the BEC wave vector. The mean value of the forward direction of the force (marked by the light blue shading in Fig. 4b) is $(9.41 \pm 0.19) \times 10^{-26}$ N. The mean value of the force along the opposite direction (the light red shading) is $(-9.47 \pm 0.17) \times 10^{-26}$ N. The measured forces along the *x*-direction are one-order-of magnitude smaller. The force variance across different periods of the square wave is $(1 \text{ to } 3) \times 10^{-53}$ N^2. These measurements confirm that our control precision for the electromagnetic forces is at the level of 10^{-27} N even in the a.c. regime.

4. Conclusion

We develop a light crystal BEC system for vectorial force sensing using quantum wave dynamics, and perform high precision measurement of two-dimensional static electromagnetic forces. Our determined force sensitivity reaches beyond the SQL well established for real-space mechanical response. We further achieve a long-term stability at the level of 10^{-28} N for measuring and controlling the force, which enables probing distant Van der Waals forces. The electromagnetic force can be well controlled in our system, enabling us to calibrate alternating forces. The BEC force sensing opens up fascinating opportunities not only for advancing fundamental science in the aspect of probing vacuum fluctuations, but also for developing atomic quantum technology such as atom-force based imaging for nanostructures.

Conflict of interest

The authors declare that they have no conflict of interest.

Acknowledgments

Author contributions

Xiaopeng Li, Xibo Zhang, and Xiaoji Zhou conceived the idea of this project and initiated the experiment. Xinxin Guo, Zhongcheng Yu, Fansu Wei, Shengjie Jin constructed the BEC sensor and performed the force measurements. All contributed to the data analysis and the writing of this manuscript.

Appendix A. Supplementary materials

Supplementary materials to this article can be found online at https://doi.org/10.1016/j.scib.2022.10.027.

References

[1] Degen CL, Reinhard F, Cappellaro P. Quantum sensing. Rev Mod Phys 2017;89:035002.
[2] Klimchitskaya GL, Mohideen U, Mostepanenko VM. The Casimir force between real materials: experiment and theory. Rev Mod Phys 2009;81:1827–85.
[3] Mohideen U, Roy A. Precision measurement of the Casimir force from 0.1 to 0.9 μm. Phys Rev Lett 1998;81:4549.
[4] Chan HB, Aksyuk VA, Kleiman RN, et al. Quantum mechanical actuation of microelectromechanical systems by the Casimir force. Science 2001;291:1941.
[5] Gangloff D, Bylinskii A, Counts I, et al. Velocity tuning of friction with two trapped atoms. Nat Phys 2015;11:915.
[6] Abbott BP, Abbott R, Abbott TD, et al. Observation of gravitational waves from a binary black hole merger. Phys Rev Lett 2016;116:061102.
[7] Arvanitaki A, Geraci AA. Detecting high-frequency gravitational waves with optically levitated sensors. Phys Rev Lett 2013;110:071105.
[8] Long JC, Chan HW, Churnside AB, et al. Upper limits to submillimetre-range forces from extra space-time dimensions. Nature 2003;421:922–5.
[9] Giessibl FJ. Advances in atomic force microscopy. Rev Mod Phys 2003;75:949–83.
[10] Binnig G, Rohrer H. In touch with atoms. Rev Mod Phys 1999;71:S324–30.
[11] Sidles JA, Garbini JL, Bruland KJ, et al. Magnetic resonance force microscopy. Rev Mod Phys 1995;67:249–65.
[12] Rugar D, Budakian R, Mamin HJ, et al. Single spin detection by magnetic resonance force microscopy. Nature 2004;430:329.
[13] Bleszynski-Jayich AC, Shanks WE, Peaudecerf B, et al. Persistent currents in normal metal rings. Science 2009;326:272.
[14] Robinson IA, Schlamminger S. The watt or Kibble balance: a technique for implementing the new SI definition of the unit of mass. Metrologia 2016;53: A46–74.
[15] Caves CM, Thorne KS, Drever RWP, et al. On the measurement of a weak classical force coupled to a quantum-mechanical oscillator. Rev Mod Phys 1980;52:341–92.
[16] Braginskiĭ VB, Vorontsov YI. Quantum-mechanical limitations in macroscopic experiments and modern experimental technique. Soviet Physics Uspekhi 1975;17:644–50.
[17] Mamin HJ, Rugar D. Sub-attonewton force detection at millikelvin temperatures. Appl Phys Lett 2001;79:3358–60.
[18] Teufel JD, Donner T, Castellanos-Beltran MA, et al. Nanomechanical motion measured with an imprecision below that at the standard quantum limit. Nat Nanotechnol 2009;4:820–3.
[19] Moser J, Güttinger J, Eichler A, et al. Ultrasensitive force detection with a nanotube mechanical resonator. Nat Nanotechnol 2013;8:493–6.
[20] Moser J, Eichler A, Güttinger J, et al. Nanotube mechanical resonators with quality factors of up to 5 million. Nat Nanotechnol 2014;9:1007–11.
[21] Rossi N, Braakman FR, Cadeddu D, et al. Vectorial scanning force microscopy using a nanowire. Nat Nanotechnol 2017;12:150.
[22] de Lépinay LM, Pigeau B, Besga B, et al. A universal and ultrasensitive vectorial nanomechanical sensor for imaging 2D force fields. Nat Nanotechnol 2017;12:156.
[23] Hebestreit E, Frimmer M, Reimann R, et al. Sensing static forces with free-falling nanoparticles. Phys Rev Lett 2018;121:063602.
[24] Schreppler S, Spethmann N, Brahms N, et al. Optically measuring force near the standard quantum limit. Science 2014;344:1486–9.
[25] Shaniv R, Ozeri R. Quantum lock-in force sensing using optical clock Doppler velocimetry. Nat Commun 2017;8:14157.
[26] Gilmore KA, Affolter M, Lewis-Swan RJ, et al. Quantum-enhanced sensing of displacements and electric fields with two-dimensional trapped-ion crystals. Science 2021;373:673–8.
[27] Rugar D, Schneeweiss P, Visanescu G, et al. Cold-atom scanning probe microscopy. Nat Nanotechnol 2011;6:346.
[28] Biercuk MJ, Uys H, Britton JW, et al. Ultrasensitive detection of force and displacement using trapped ions. Nat Nanotechnol 2010;5:646–50.
[29] Blums V, Piotrowski M, Hussain MI, et al. A single-atom 3D sub-attonewton force sensor. Sci Adv 2018;4:eaao4453.
[30] Gustavsson M, Haller E, Mark MJ, et al. Control of interaction-induced dephasing of Bloch oscillations. Phys Rev Lett 2008;100:080404.
[31] Aidelsburger M, Atala M, Lohse M, et al. Realization of the Hofstadter Hamiltonian with ultracold atoms in optical lattices. Phys Rev Lett 2013;111:185301.
[32] Miyake H, Siviloglou GA, Kennedy CJ, et al. Realizing the Harper Hamiltonian with laser-assisted tunneling in optical lattices. Phys Rev Lett 2013;111:185302.
[33] Ferrari G, Poli N, Sorrentino F, et al. Long-lived Bloch oscillations with Bosonic Sr atoms and application to gravity measurement at the micrometer scale. Phys Rev Lett 2006;97:060402.
[34] Poli N, Wang F-Y, Tarallo MG, et al. Precision measurement of gravity with cold atoms in an optical lattice and comparison with a classical gravimeter. Phys Rev Lett 2011;106:038501.

[35] Zhou M-K, Hu Z-K, Duan X-C, et al. Precisely mapping the magnetic field gradient in vacuum with an atom interferometer. Phys Rev A 2010;82:061602.

[36] Wood AA, Bennie LM, Duong A, et al. Magnetic tensor gradiometry using Ramsey interferometry of spinor condensates. Phys Rev A 2015;92:053604.

[37] Gosar K, Arh T, Meznarsic T, et al. Single-shot Stern-Gerlach magnetic gradiometer with an expanding cloud of cold cesium atoms. Phys Rev A 2021;103:022611.

[38] Tang P, Peng P, Li Z, et al. Parallel multicomponent interferometer with a spinor Bose-Einstein condensate. Phys Rev A 2019;100:013618.

[39] Hu D, Niu L, Jin S, et al. Ramsey interferometry with trapped motional quantum states. Commun Phys 2018;1:29.

[40] Jin S, Guo X, Peng P, et al. Finite temperature phase transition in a cross-dimensional triangular lattice. New J Phys 2019;21:073015.

[41] Jin S, Zhang W, Guo X, et al. Evidence of potts-nematic superfluidity in a hexagonal sp^2 optical lattice. Phys Rev Lett 2021;126:035301.

[42] Ludlow AD, Zelevinsky T, Campbell GK, et al. Sr lattice clock at 1×10^{-16} fractional uncertainty by remote optical evaluation with a Ca clock. Science 2008;319:1805.

[43] Kinoshita T, Wenger T, Weiss DS. All-optical Bose-Einstein condensation using a compressible crossed dipole trap. Phys Rev A 2005;71:011602.

Xiaopeng Li is a professor of Physics at Fudan University. He received his Ph.D. degree from University of Pittsburgh in 2013 and joined Fudan University as a faculty member in 2016 after three years at University of Maryland, supported by a JQI theoretical postdoctoral fellowship. He has been a full professor since 2019. He is active in quantum information science and condensed-matter theories, with his primary research interest in exploiting the computation power of various quantum simulation platforms.

Xinxin Guo received his Ph.D. degree from Peking university in 2022. His research interest focuses on cold atom and precision measurements.

Xibo Zhang received his Ph.D. degree in 2012 at the Department of Physics, University of Chicago. He became a faculty member of International Center for Quantum Materials, School of Physics, Peking University in 2015. His research interest includes quantum simulation using ultracold atoms, quantum many-body physics, and ultra-stable laser precision spectroscopy.

Zhongcheng Yu is now a Ph.D. candidate at School of Electronics, Peking University. His research focuses on the quantum simulation based on ultracold atoms, dynamic evolution and high-orbit physics in optical lattices.

Xiaoji Zhou obtained his Ph.D. degree from Peking University in 2001. He is now a professor at School of Electronics, Peking University. His research interest focuses on coherent manipulation of the ultracold atoms, quantum simulation based on optical lattices, and quantum precision measurements.